In situ diode laser absorption measurements of plasma species in a gaseous electronics conference reference cell reactor

Daniel B. Oh and Alan C. Stanton
Southwest Sciences, Inc., 1570 Pacheco St., Suite E-11, Santa Fe, New Mexico 87505

Harold M. Anderson and Michael P. Splichal
Department of Chemical and Nuclear Engineering, The University of New Mexico, Albuquerque, New Mexico 87131

(Received 21 April 1994; accepted 28 January 1995)

A major objective of the microelectronics industry is to perfect methods for controlling dimensional accuracy during plasma etching of submicron features in wafer substrates. Optical sensors as monitors of gas phase etch chemistry are attractive because they offer the potential of nonintrusive *in situ* measurements for use as real time inputs to process control. In this study, infrared lead-salt diode lasers are used to probe fluorocarbon-based plasmas used for etching of silicon and silicon dioxide in a gaseous electronics conference reference cell reactor. The diode laser sensor is used for *in situ* measurements of neutral CF_2 reactive intermediates and CF_2O etch product. Possible correlations between etch process outcomes and parameters measured by diode laser absorption are identified. The diode laser measurement of CF_2 concentration is found to be possibly useful as an indicator of etch rates or selectivity. In addition, diode laser monitoring of CF_2O during etching of SiO_2 is potentially useful as an end point monitor. Further research and development based on these results are expected to lead to new process control strategies for improved reliability and product yield in plasma etching.

I. INTRODUCTION

The development of real-time process control for semiconductor device fabrication is critical to advancing the state of the art in manufacturing microelectronic circuits. In the area of plasma etching and related technologies, the corrosive environment of the plasma reactors and the need for real-time response suggest the application of nonintrusive optical monitors of plasma parameters might offer promising approaches for achieving process control. Optical emission spectroscopy has been used with some success, in that apparent correlations between atomic emission intensities and macroscopic etching characteristics have sometimes been found. Some laser-based monitoring techniques have been used in plasma etching research, but most of these techniques (such as laser induced fluorescence) are too expensive and limited in application to see practical widespread use as a process monitor.

This study exploits recent improvements in tunable diode laser operating characteristics and advances in technology for measuring small absorbances with these lasers to implement compact and cost effective instrumentation for plasma process monitoring. Specifically, single mode liquid-nitrogen cooled lead-salt lasers, combined with high frequency wavelength modulation spectroscopy, provide a means for quantitative, real-time *in situ* detection of important plasma species. By selectively using the diode lasers to detect plasma parameters that are inaccessible to optical emission spectroscopy, and combining this information with optical emission data and measurements of plasma electrical characteristics, we believe that more effective means of process control can be devised. In particular, diode laser absorption can measure ground state species, while optical emission measures only excited state species that may not be relevant to process chemistry.

In our initial research, we have focused on fluorocarbon-based plasmas such as those used in the etching of silicon, oxides, certain metals, and silicides. A prototype diode laser sensor is used for *in situ* measurements of CF_2 and CF_2O in a reference plasma reactor [the "gaseous electronics conference (GEC) reference cell reactor"]. Measurements of carbonyl fluoride (CF_2O) are made to study possible end point detection in etching SiO_2 over poly-Si. The CF_2 measurements are compared with SiO_2 and poly-Si etch rates and etch selectivity.

In situ measurements in low pressure process plasmas using diode laser absorption have been reported previously. Gas temperature and absolute concentrations of atomic chlorine in Cl_2 discharges were measured by Wormhoudt *et al.* using lead-salt laser absorption near 882 cm^{-1}.[1] This technique was used by Richards *et al.* to investigate the utility of optical emission actinometry for measuring Cl atom concentrations by comparison with direct diode laser measurements of Cl.[2] A particular result of their work was the finding that actinometry cannot be used to measure trends in atomic chorine concentration in Cl_2 plasmas.[2] To obtain adequate sensitivity in this previous work, multiple pass optics internal to the reactor were used to achieve a total absorption path length in the discharge of about 250 cm. By contrast, the high sensitivity achieved in the present work using high frequency wavelength modulation spectroscopy eliminates the need for multiple pass optics and permits the use of a single optical pass.

Diode laser measurements of CF_x and SiH_x radicals in low pressure plasmas have been reported by researchers at Nagoya University.[3–6] The absolute concentrations of radical

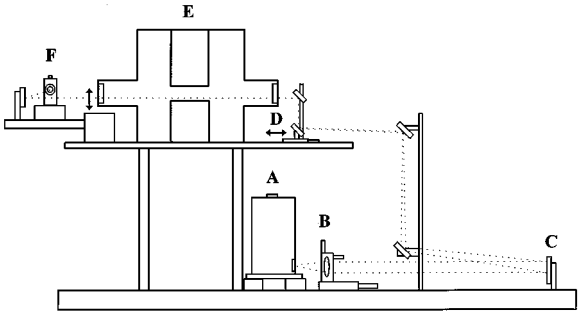

FIG. 1. Optical setup for *in situ* measurements in the plasma reactor using the diode laser sensor. A: Liquid N_2 Dewar/diode laser; B: ZnSe collimating lens; C: focal length=200 cm mirror; D: focal length=15 cm mirror; E: GEC Reference Cell Etching Reactor; F: HgCdTe detector.

and product species, including CF_2, in low pressure rf plasmas have been measured by Wormhoudt using diode laser absorption.[7] In all of these studies internally mounted multiple pass mirrors are used to attain very long absorption path lengths. *In situ* measurements in process plasmas using lead-salt diode lasers are also in progress in at least two other research groups.[8,9] In particular, diode laser measurements of relative concentrations of CF_2 and CF_3 in low pressure C_2F_6 discharges have been reported recently by Sun *et al.*[10] A single pass optical configuration is used in their work.

II. EXPERIMENTAL METHODS

A. Diode laser detection system

The lead-salt diode laser system has been used in several prior studies at Southwest Sciences Inc., which have focused on optimization of detection methods for trace gases in atmospheric chemistry and combustion.[11,12] The diode lasers are mounted on a temperature-controlled copper block in a commercially available liquid-nitrogen (LN_2) Dewar (Laser Photonics). The laser optical output is transmitted through a barium fluoride window mounted on the Dewar housing. Four diode lasers may be mounted in the Dewar at the same time. A resistive heater bonded to the copper block is used to heat the lasers above LN_2 temperature for coarse tuning of the laser wavelength, with temperature control provided by a commercial *p-i-d* controller (Lakeshore Cryotronics). High resolution tuning of the laser wavelength is provided by a low-noise battery powered current supply (ILX Lightwave).

Two diode lasers, both buried double heterostructure devices (Fujitsu) manufactured by liquid phase epitaxy, are used in this study. One of these lasers may be temperature tuned from approximately 1200 to 1300 cm^{-1}, which is a spectral region appropriate for detection of CF_4, CF_3, CF_2 (ν_1 band), CF, and CF_2O. This laser is used in the present work to detect CF_2O. The second laser is tunable from 1040 to 1120 cm^{-1}. This laser accesses the stronger ν_3 absorption band of CF_2 and is used for the CF_2 measurements in this study.

The optical setup for the *in situ* measurements in the plasma reactor is shown in Fig. 1. The diode laser output, which is highly divergent as it emerges from the Dewar, is collimated into a relatively wide diameter ($\sim$1 to 2 cm) beam using a ZnSe aspheric lens. Aside from this lens, only reflective optics are used in the system. A system of mirrors is used to condense the collimated beam to a diameter of about 1 to 2 mm and direct it across the plasma reactor in a single optical pass. The transmitted beam is focused onto a fast photovoltaic HgCdTe detector (liquid-nitrogen cooled). The system is designed so that the line of sight can be positioned at various locations across the 2.5-cm interelectrode gap in the reactor by translation of mirror ''D'' as shown in Fig. 1. The detector and final focusing mirror are mounted on a platform that can be translated vertically into alignment with the transmitted diode laser beam. A co-aligned helium neon laser is used to set and verify the position of the absorption line of sight. For these initial experiments, the diode laser probes a line of sight approximately 3 mm above the wafer (powered electrode) surface.

This simple single pass design is possible because of the very high detection sensitivity that can be achieved using high frequency laser wavelength modulation techniques, briefly described below. As a consequence, no multiple pass mirrors are required which would otherwise need to be mounted inside the reactor. Substantially improved spatial resolution is possible when the diode laser sensor is configured for a single optical pass. Also, the single frequency (single longitudinal mode) characteristic of the lasers over much of their operating ranges eliminates the need for a monochromator to filter unwanted wavelengths, and the compact, inexpensive liquid-nitrogen Dewar replaces the costly and bulky closed cycle helium refrigerator that was required to cool older lead-salt laser devices.

High frequency laser wavelength modulation spectroscopy (WMS) is used to process the absorption signals observed in these experiments. We have described this technique in considerable detail in two recent publications, including comparisons with other high frequency diode laser detection methods (e.g. one- and two-tone frequency modulation spectroscopy).[11,13] Briefly this method, which is an extension of diode laser ''derivative spectroscopy'' techniques, widely used at kHz frequencies,[14] involves superposition of a small sinusoidal modulation on the diode laser injection current. Typically, the amplitude of the current modulation is chosen so that the induced wavelength modulation is comparable to the width of the spectral feature under study. Phase-sensitive electronics are then used to demodulate the detector photocurrent at the modulation frequency, f, or a harmonic, nf. By implementing this technique at sufficiently high frequencies, laser noise is minimal and detector-limited (ideally, shot noise–limited) sensitivity can be achieved. Our studies have shown that detection frequencies as low as 100 kHz are often sufficient to achieve these objectives, although the optimum frequencies are laser dependent. The distinction between WMS and frequency modulation (FM) spectroscopy (as described, for example, in Ref. 15) is mostly semantic—FM spectroscopy is defined as using modulation frequencies comparable to or greater than the absorption linewidths (50 MHz or greater for the present experiment), whereas WMS uses modulation frequencies much smaller than the absorption linewidths.

In the present work, we use 50 kHz modulation with second harmonic detection. The 50 kHz sine wave for laser current modulation is generated by a Wavetek Model 191 signal generator and fed to the external modulation input of the ILX laser current controller. The detector output is bandpass-filtered and amplified and sent to a Stanford Research Systems SR530 lock-in amplifier operating in the $2f$ mode. The lock-in amplifier is specially modified to bypass the usual time constant filtering and exhibits an effective time constant of <5 μs. This arrangement allows us to take advantage of the optimized mixer and low noise narrow bandwidth amplifier in the SR530. The 50 kHz modulation frequency is the highest frequency accepted by the SR530 for $2f$ operation. The lock-in analog output is low pass–filtered (Stanford Research Model SR560 low noise preamplifier) before digitization.

The microcomputer-based data acquisition system uses a high speed analog-to-digital (A/D) converter board (Analog Devices RTI-860) to digitize the lock-in output. The laser wavelength is repetitively scanned with an analog voltage ramp generated by a programmable waveform synthesizer board (QuaTech WSB-10). Each A/D cycle is synchronized with the repetitive scanning of the laser wavelength for rapid averaging of the $2f$ signals. Typical parameters for a single scan are 512 or 1024 data points, with a dwell time of 20 μs per data point. For most data taken in this study, 1000 such scans are co-added. The effective measurement bandwidth is given by the product of the dwell time and the number of scans and is 50 Hz for these experiments. Ideally, measurements made using longer averaging times should show system noise decreasing with the square root of the integration time. In the present instance, however, sensitivity is limited by accidental etalon effects arising due to optical interference of scattered laser light with the primary beam, and no advantage is gained by using longer signal averaging times. The etalon effects are substantially reduced in the time-averaged signals by using low frequency ($\sim$25 Hz) translation of some of the mirrors in the optical train for asynchronous variation of the optical path differences that give rise to the etalon fringes.[16] Several other methods for reducing the undesired etalon fringe effects in diode laser experiments have been described in the literature.[17–19]

B. Reference cell reactor

The plasma etching reactor used in these studies is based on a ''reference cell'' concept developed at a 1988 Gaseous Electronics Conference (October 18–22, Minneapolis, MN) workshop on the ''Design, Calibration, and Modeling of Research RF Plasma Processing Systems.'' The objective in establishing a reference cell design is to facilitate comparison of research results obtained in different laboratories, such that processes or diagnostics can be easily transferred from one system to another. These ''GEC Reference Cell Reactors'' are currently in use in several industrial, government, and academic research laboratories.[20]

The GEC Reference Cell Reactor design features include: (1) two 8-inch, two 6-inch, and four 2.75-inch ports for optical diagnostic measurements; (2) gas injection through a showerhead electrode; (3) interchangeable water-cooled electrodes; (4) symmetrical pumpout of the inlet gas through a dual exhaust manifold; (5) ability to ground, float, or bias each electrode independently; (6) movable electrode assembly allowing 0.5- to 2.5-inch interelectrode spacings; and (7) UHV flange construction to insure base pressure less than 10^{-7} Torr. A standard configuration with 4-inch diameter aluminum electrodes, Teflon insulators, and a 1-inch interelectrode spacing is used for all of the experiments reported here.

Prior to these studies, the University of New Mexico (UNM) reactor was equipped for electrical characterization of the plasma as part of an interlaboratory comparison study on the electrical characteristics of processing plasmas.[20] This equipment was designed to analyze the entire rf waveform driving the plasma, including higher harmonics of the 13.56-MHz applied rf voltage. A complete description of the electrical characterization of the plasma can be found elsewhere.[20–22] These same electrical characterization procedures are followed in the present experiments.

The UNM GEC Reference Cell Reactor is also equipped with a spatial and spectral imaging system for optical emission measurements. This system comprises a Princeton Instruments thermoelectrically cooled charge-coupled device (CCD) detector matched to a Chromex 250IS toroidal mirror imaging spectrometer. Coupled to the entrance slit of the spectrometer is a bundle of 200-μm diameter quartz optical fibers each fitted with a quartz focusing lens to collect optical emission from the plasma. In this system, light from the discharge is sampled along parallel paths at different positions between the electrodes. The emission is collected through one of the 8-inch optical ports on the reactor, which is fitted with a quartz window for transmission down to 190 nm. Light collected from each fiber is dispersed in the spectrometer and imaged on parallel strips of diodes on the uv-sensitive CCD detector. In this fashion, spatially resolved optical emission from various heights across the interelectrode gap is collected and analyzed. The CCD camera and spectrometer are both controlled by a microcomputer. Optical emission data from the CCD detector are updated every 200 ms so that the emission is both time and space resolved. Low resolution, 150- line/mm gratings are used for these studies in order to maximize the wavelength range of optical emission collected during a plasma etch cycle.

In the present experiments, optical emission and diode laser absorption data are collected simultaneously as illustrated in Fig. 2. Three of the optical fibers for the emission system sample emission through the 8-inch port, while the single pass diode laser absorption measurements are made using two opposing 2.75-inch optical ports fitted with IR-transmitting barium fluoride windows. The diode laser system is aligned to probe a line of sight on the same horizontal plane as one of the optical emission channels, approximately 3 mm above the wafer, as verified by the helium neon alignment lasers used for both optical systems. With the exception of data relating to end point detection, the optical emission data are not presented here. A separate publication reporting the results of a chemometrics-based analysis that relates the optical emission and diode laser absorption data to process parameters is planned.

The reactor gas handling system includes CF_4, CF_3H, Ar,

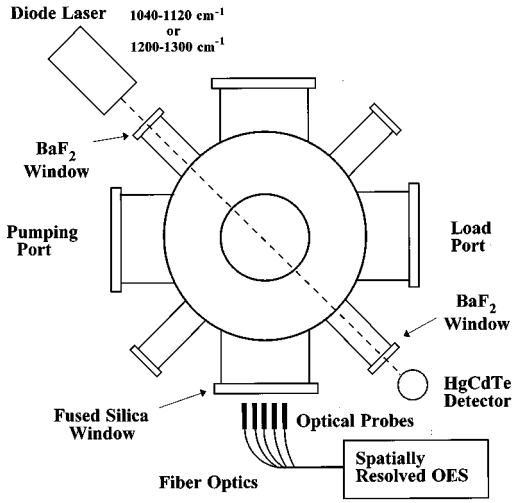

FIG. 2. Schematic diagram of the diode laser and optical emission diagnostics in the GEC Reference Cell Reactor. One of the optical emission probes is aligned to sample the same horizontal plane that the diode laser beam probes, which is about 3 mm above the wafer.

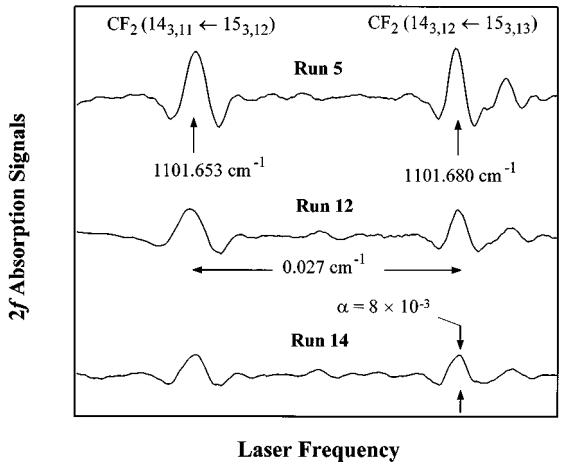

FIG. 3. Absorption spectra of CF_2 under three different rf discharge conditions in the GEC Reference Cell Reactor; Run (5) 33.3% CF_3H/66.7% CF_4, 500 mTorr, 500 V peak-to-peak rf voltage; run (12) 4.8% CF_3H/95.2% CF_4, 500 mTorr, 500 V peak-to-peak rf voltage; run (14) 4.8% CF_3H/95.2% CF_2, 700 mTorr, 700 V peak-to-peak rf voltage. See Table I for the summary of experimental conditions of 15 runs.

and O_2 feed gases. All gases are high purity electronic grade. Gas flow rates are controlled by thermal conductivity-type mass flow controllers and constant pressure is maintained by an automatic throttling valve on the pumpout line controlled by capacitance manometer pressure transducers. The reactor is designed to accommodate up to 4-inch wafers for single wafer plasma etching. The lower electrode where the wafer is located is the powered electrode for these studies, so that processing conditions are typical of the reactive ion etching (RIE) mode. Wafers are etched in CF_4/CF_3H discharges while the process is probed simultaneously with the optical emission and diode laser absorption sensors. Between etching cycles, the chamber is subjected to an O_2 plasma clean cycle in order to restore the chamber condition to its original state.

Two types of wafers were used in this study, a blanket thermal oxide wafer for endpoint determination, and a half-and-half oxide/poly-Si wafer for selectivity determination. The blanket oxide wafers were lightly doped ⟨100⟩ *n*-type Si wafers with 8,000 to 10,000 Å of a thermal oxide layer. The selectivity wafers were lightly doped ⟨100⟩ *p*-type with half of the wafer coated with 8,000 to 10,000 Å of a thermal oxide layer and the other half with a poly-Si over oxide layer. The selectivity wafers were also coated with a very open patterned layer of photoresist (5,000 Å). Film thicknesses for the selectivity wafers were measured before and after etching with a Nanospec interferometer accurate to ~10 Å. The blanket wafers were etched to endpoint.

III. RESULTS AND DISCUSSIONS

A. *In situ* measurement of CF_2

To investigate the possible application of an *in situ* diode laser measurement of CF_2 in monitoring etch rate or etch selectivity, a set of 4-inch selectivity wafers was prepared for processing in the GEC Reference Cell Reactor. Enough wafers (15) were prepared to conduct a 3-factor, 3-level Box Behnken factorial designed experiment. The experimental processing conditions were chosen to define a wide range of the potential reactor operational space, and hence, a significant range of response in the observed plasma chemistry and etch outcomes. Factors included in the design were percent CF_3H in the CF_4/CF_3H feed, peak-to-peak applied rf voltage, and total chamber pressure.

Figure 3 shows three CF_2 absorption spectra taken *in situ* under different discharge conditions in the GEC Reference Cell Reactor. The spectral region scanned is in the *P* branch of the υ_3 band of CF_2 near 1101 cm^{-1}.[23,24] The absorption features are recorded using the 100-kHz $2f$ detection method described earlier. The advantages of this technique, which can be readily extended into the MHz regime by using discrete rf components (mixers, filters, etc.) in place of the lock-in amplifier, are that detection occurs at frequencies beyond significant "$1/f$" laser noise, and the signal baseline is flat. The two prominent CF_2 absorption features in Run 14 of Fig. 3 correspond to a peak absorbance of about 8×10^{-3}, while the regular, high frequency features in the signal baselines arise from unintended etalon fringes. In addition to the strong absorption features due to CF_2, there are hints of weaker absorption features that may correspond to other species present in the plasma including CF_3.

The experimental conditions and results (measured etch rates) for the 15 etching experiments are listed in Table I. Shown in Figs. 4 and 5 are plots of the observed SiO_2 and poly-Si etch rates versus the diode laser CF_2 absorption feature intensity (proportional to CF_2 concentration) for each of the conditions listed in Table I. A *P*-branch line of CF_2, which we identify as the $14_{3,12}\leftarrow 15_{3,13}$ transition near 1101.68 cm^{-1}, is used for monitoring CF_2 concentration in these measurements. The spectroscopic identification of the CF_2 absorption line is made by comparing the observed spectra with tabulated line positions provided by Burkholder.[25]

TABLE I. Summary of experimental conditions, measured DC bias, and measured etch rates for the etch selectivity experiments.

Run No.	Pressure (mTorr)	Peak-to-Peak voltage (V)	Percent CF_3H	Flows (CF_4/CF_3H) (sccm)	Calculated power (W)	DC self-bias (V)	CF_2 signal (arb. units)	Oxide etch rate (nm/min)	Poly-Si etch rate (nm/min)	Oxide/poly-Si selectivity
1	500	504	33.3	40/20	26.2	−154.3	17.2	9.28	1.30	7.2
2	300	900	21.6	40/11	58.3	−403.1	6.64	91.4	59.0	1.6
3	700	508	21.6	40/11	32.8	−145.3	14.1	10.3	3.70	2.8
4	500	900	4.8	40/2	74.0	−399.0	4.66	98.3	94.1	1.1
5	500	508	33.3	40/20	26.3	−152.8	17.2	11.2	3.67	3.1
6	300	504	21.6	40/11	23.3	−176.3	14.9	17.4	10.8	1.6
7	500	704	21.6	40/11	50.6	−256.2	11.4	44.5	30.5	1.5
8	300	712	33.3	40/20	38.9	−289.2	10.5	46.4	25.1	1.9
9	700	912	21.6	40/11	120.5	−350.4	2.88	177	115	1.5
10	700	704	33.3	40/20	60.4	−226.4	12.4	41.8	17.9	2.3
11	300	704	4.8	40/2	41.2	−271.1	7.27	47.0	47.6	1.0
12	500	504	4.8	40/2	30.5	−139.9	9.41	15.4	16.8	0.9
13	500	900	33.3	40/20	84.8	−357.3	5.47	114	61.0	1.9
14	700	704	4.8	40/2	57.5	−243.2	6.66	47.1	50.5	0.9
15	500	704	21.6	40/11	52.6	−243.9	7.27	47.9	32.5	1.5

Figures 4(a) and 5(a) show that the etch rates for both films have a generally inverse correlation with the CF_2 concentration as measured by diode laser absorption. Scatter in both sets of data is largely attributable to the simultaneous variation of each of the experimental factors in this factorially designed experiment. For example, different combinations of CF_2 density and DC self-bias may lead to essentially the same etching rate for either substrate. The DC bias is a function of all three controlled variables (CF_3H percent, applied voltage, and pressure) in this study.

The apparent inverse correlation between etch rates and CF_2 concentration is interesting, but it is clearly not sufficient in itself to serve as a basis for process control. In Figs. 4(b) and 5(b), we again plot SiO_2 and poly-Si etch rates, but now versus the CF_2 signal normalized by DC self-bias. A physical basis for this normalization may be rationalized by thinking of CF_2 as an inhibitor to etching through polymer formation,[26] while DC self-bias may be viewed as an indicator of ion bombardment energy,[27] where higher etch rates are expected under conditions of higher DC self-bias. We find that plotting etch rates versus this normalized parameter produces a steeper (at higher etch rates) and smoother correlation that may be more suitable for use in process control applications.

Perhaps a more important parameter from the process control perspective is etch selectivity. The present data indi-

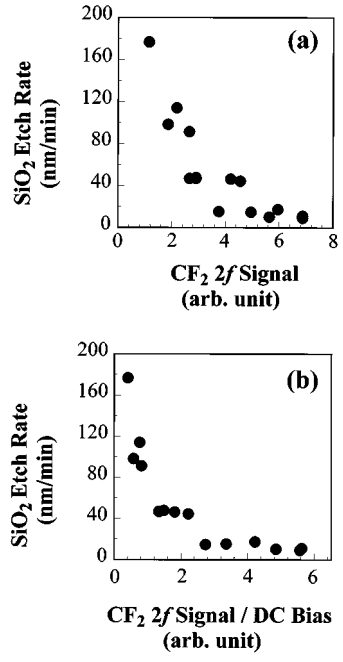

FIG. 4. Etch rates of SiO_2 plotted against (a) the CF_2 absorption signal (arbitrary units) and (b) the CF_2 absorption signal normalized by DC self-bias. The CF_2 concentration is directly proportional to the absorption signal.

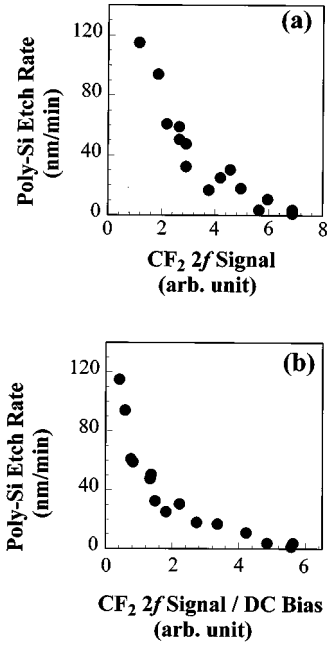

FIG. 5. Etch rates of poly-Si plotted against (a) the CF_2 absorption signal (arbitrary units) and (b) the CF_2 absorption signal normalized by DC self-bias.

cate a small but suggestive increasing trend toward higher selectivity in etching SiO_2 (as quantified by the ratio of SiO_2 to Si etch rates) at higher CF_2 concentrations. While many details of the fluorocarbon discharge etch mechanism remain unknown, a widely accepted qualitative description of the process has emerged.[26] Etching of SiO_2 appears to occur as a result of a thin fluorocarbon film (<10 Å) which is formed on the substrate surface from impinging unsaturated CF_x radicals. As fresh CF_x radicals are continuously added to the film from the gas phase, material from the carbonaceous layer is gasified by ion-induced reactions with the underlying SiO_2 substrate. Naturally, fluorocarbon layers also form on exposed Si during etching, but since no oxygen is present in the substrate, a fairly thick (~100-Å) film accumulates on the Si, blocking the etch process and producing a selective etch.[28] High selectivity in the SiO_2 etch is generally believed to require high CF_2 concentrations, but high CF_2 concentration alone may not necessarily result in high selectivity. The range of etching conditions in this study did not clearly establish the transition from low to high etch selectivity, and additional experiments are planned to address this point more clearly.

We are also exploring chemometrics-based analyses to identify correlations between process outcomes and diode laser or optical emission measurements. Our preliminary efforts in this area are encouraging in that stronger correlations with selectivity are obtained by utilizing spectral information from extended wavelength scans of the diode laser that may include absorption features of other species besides CF_2. We plan to describe these analyses in a separate publication.

The absolute number densities of CF_2 that we observe in these experiments can be estimated from the measured absorbances given knowledge of the absorption path length, the temperature, and the absorption cross section for the particular CF_2 line. Experimental values for the CF_2 infrared band strengths are available[29–31] which can be used to derive a reliable estimate of the absorption cross section for a given line. The strength of an individual absorption line may be estimated from the relation

$$S_{\text{line}}/S_{\text{band}} \simeq A g_{NK} \exp(-E_{\text{rot}}/kT)/Q_{\text{rot}}, \tag{1}$$

where A is the Hönl-London factor, g_{NK} is the lower state degeneracy, E_{rot} is the energy of the lower state, and Q_{rot} is the rotational partition function. Using the classical approximation for Q_{rot} and assuming the symmetric rotor value for the Hönl–London factor,[32] we obtain $S_{\text{line}}/S_{\text{band}} \simeq 0.0021$ for the $14_{3,12} \leftarrow 15_{3,13}$ transition at $T=300$ K. Suto and Steinfeld have obtained an experimental value of $S_{\text{band}}=2.8 \times 10^{-17}$ cm^2 molecule^{-1} cm^{-1} for the υ_3 band of CF_2.[31] Thus we estimate $S_{\text{line}}=5.8\times10^{-21}$ cm^2 molecule^{-1} cm^{-1} at $T=300$ K for the CF_2 line monitored in the etching experiments. The absorption cross section at line center for this line under room temperature Doppler-broadened conditions is $\sigma_0=2.8\times10^{-17}$ cm^2 molecule^{-1}.

From prior studies of low pressure discharges, the translational-rotational temperature is expected to be somewhat elevated above room temperature in the discharge region. For example, Maruyama, Sakai, and Goto report a CF rotational temperature of 350±40 K in a low pressure CF_3H plasma based on diode laser measurements of the relative intensities of several CF lines originating from different rotational states.[33] In the present study, the limited single mode tuning characteristics of the diode laser used for CF_2 detection did not permit a sufficiently extended wavelength scan for measurement of CF_2 rotational temperature. Although we did not measure the CF_2 absorption linewidths, the $2f$ line shapes did not appear significantly broadened in the discharge spectra compared to the line shapes observed in preliminary spectra taken of CF_2 generated in a microwave discharge. In these latter experiments, measurements were made well downstream of the discharge where the discharge products were thermalized with a room temperature bath gas. For present purposes of estimating CF_2 concentrations, we believe a reasonable approximation is to use $T=300$ K in evaluating the CF_2 cross section. We note that even at a temperature of 500 K, the line center absorption cross section for the CF_2 line that we measured is reduced only by a factor of 2 relative to its room temperature value.

From Beer's law, the CF_2 concentration is

$$[CF_2] = \alpha/\sigma_0 l, \tag{2}$$

where α is the measured absorbance, σ_0 is the line center cross section estimated above, and l is the absorption path length. Gas phase reactions for removal of CF_2 under the experimental reactor conditions are very slow, so that we expect that significant CF_2 concentrations are present outside the active plasma region. Taking $l=45$ cm (the spacing between the reactor windows), the line-of-sight averaged CF_2 concentration is $[CF_2]=7.9\times10^{14}$. From the observed absorbances, we estimate that the CF_2 concentrations in the series of 15 etching experiments ranged approximately from 5×10^{12} cm^{-3} to 3×10^{13} cm^{-3}.

Although *relative* CF_2 concentrations in low pressure fluorocarbon process plasmas have been measured in a number of previous studies using laser induced fluorescence (LIF), absolute number densities have rarely been assigned due to the experimental difficulties in calibrating LIF signals. Buchmann *et al.* estimate a CF_2 concentration of ~2.5×10^{13} cm^{-3} from LIF measurements performed in a 40-mTorr CF_4/O_2 rf plasma, with 2% O_2 in the feed gas.[34] Kinetic modeling calculations by Ryan and Plumb predict CF_2 concentrations in the range of 10^{14} cm^{-3} for 500-mTorr CF_4 plasmas.[35] Wormhoudt reports CF_2 concentrations ranging from about 2×10^{12} to 1.5×10^{13} cm^{-3} in his diode laser studies of a low pressure CF_4 rf plasma,[7] and CF_2 number densities in the high 10^{12}-cm^{-3} range in a C_2F_6 plasma are estimated by Sun *et al.* from their diode laser measurements.[9] In contrast to the relatively high concentrations estimated in the present work and in these prior studies, Hargis, Light and Gee report much lower CF_2 concentrations in their LIF measurements in CF_3H discharges, ranging from about 10^{10} cm^{-3} to 1.6×10^{11} cm^{-3}.[36]

B. Etch product detection

We also searched for diode laser absorption features that could be attributed to gas phase etch products. This search is made by examining *in situ* spectra taken in various wave-

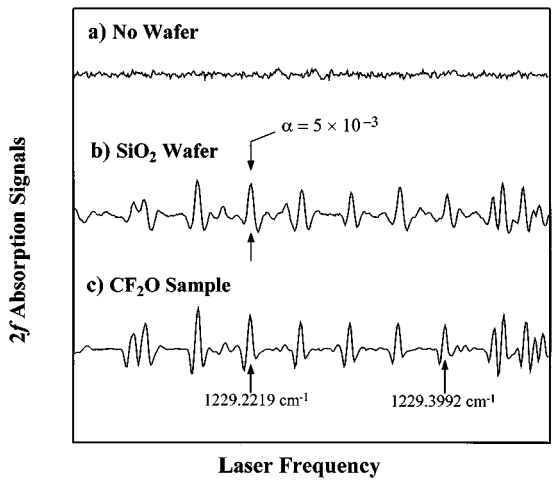

FIG. 6. *In situ* detection of CF_2O product in etching of SiO_2; a) discharge absorption spectrum with no wafer, b) spectrum with SiO_2 wafer present, c) laboratory spectrum of CF_2O.

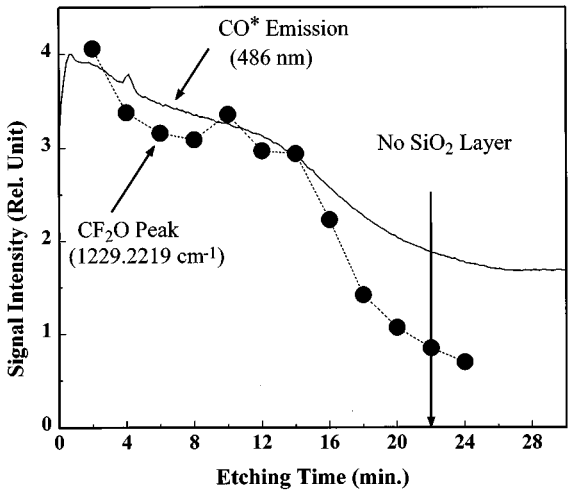

FIG. 7. Comparison of the time dependence of CO^* emission (486 nm) and CF_2O absorption during etching of an SiO_2 wafer. The etching conditions are 4.8% CF_3H/95.2% CF_4, 500 mTorr, 700 V peak-to-peak rf voltage.

length regions accessible within the temperature/current operational space of the two diode lasers. Absorption spectra obtained under etching conditions (with a wafer present) are compared with spectra obtained when the discharge is operated with no wafer present. Absorption signals that appear only when etching occurs are indicative of an etch product. Such a comparison is presented in Fig. 6, which shows absorption spectra taken in the 1230-cm^{-1} region. Trace (a) is a spectrum taken with no wafer present, whereas trace (b) is taken under etching conditions. Except for the addition of the wafer, the reactor operating conditions are identical for the two traces (13% CF_3H/87% CF_4, 500 mTorr, 700 V peak-to-peak rf voltage).

We identify the product detected in this manner as CF_2O (carbonyl fluoride). This species is known to be a product of SiO_2 etching in fluorocarbon discharges.[37] We have confirmed this identification by measuring absorption spectra in a sample of CF_2O obtained commercially and comparing these spectra with the etch product spectra observed in the reactor. Trace (c) in Fig. 6 is a laboratory diode laser spectrum of pure CF_2O ($\sim$0.5 Torr, 11 cm path length). The same pattern of prominent absorption features is evident in both the etch product spectrum, trace (b), and the laboratory CF_2O spectrum, trace (c). Weak absorption lines that may be present in trace (a) of Fig. 6, where no wafer is present, are likely due either to CF_2 or CF_3, or possibly CF_4 feed gas. The carbonyl fluoride lines shown in these experimental spectra are in the P-branch region of the ν_4 band of CF_2O. We have been able to assign these lines by comparison with the tabulated CF_2O spectra contained in the HITRAN infrared line parameters compilation.[38] These tabulated spectra are based on the high resolution Fourier transfrom IR data of Camy-Peyret *et al.*[39]

The possible utility of CF_2O absorption as an end-point monitor is indicated in Fig. 7, which shows a plot of the absorption intensity versus time of a CF_2O absorption line (1229.2219 cm^{-1}) as a blanket SiO_2 wafer is etched through to clearing of the film. Also shown in Fig. 7 is the time dependence of the CO^* emission signal, which is often used as an end-point monitor in selective oxide etching, monitored at 486 nm using an optical emission spectrometer as shown in Fig. 2. The CO^* emission profile shows a generally decreasing trend, leveling off to a constant emission level due to the background continuum emission of the plasma. The CF_2O absorption signal shows a similar trend, indicating that both the CO^* and CF_2O signal are generally following the evolution of etch products. The absence of a sharp drop in intensity for either signal at the end point reflects the poor spatial uniformity of the GEC Reference Cell Reactor etching characteristics. This nonuniformity is attributed to the 1-inch electrode gap and the nonuniform pattern of gas flow which results in a bulls eye pattern of wafer etching. A strong clearing of the oxide film was observed first at the perimeter of the wafer followed by slower clearing toward the center.

The similarity in the time dependence of the CF_2O absorption and CO emission signals indicates that the CF_2O signal could be useful as an end point detector in situations where simply following optical emission might fail. Such a situation might arise in a real manufacturing environment because other additives may be included in the feed gas mixture. Such additives can lead to additional emission features that may obscure the features due to etch products or contribute to the underlying emission continuum. If the contrast between the CO^* (or other etch product) emission signal and the underlying continuum emission is insufficient, the monitored emission signal can level off before the end point is reached. Although contrast may be enhanced by improving resolution, such enhancement comes at the expense of signal level.

The considerations that apply to diode laser-based end point monitoring are different. Here, the very high inherent spectral resolution of the technique and the availability of numerous candidate absorption lines of molecular etch products like CF_2O virtually guarantee that suitable interference-free monitoring lines can be identified even when other discharge species have overlapping absorption bands. Thus,

contrast of the monitored signal relative to an interfering background is not an issue, and the ultimate utility of the technique is determined by signal-to-noise considerations in measuring small absorbances.

In ongoing work, we are comparing the sensitivities of diode laser-based end point monitoring and emission-based monitoring. Preliminary experiments in the GEC Reference Cell using patterned wafers with 5% SiO_2 coverage indicate that diode laser measurement of CF_2O is sufficiently sensitive for end point monitoring even at this reduced level of product concentration. We are also examining diode laser measurement of other etch product species (e.g., CO, CO_2) that are potential end point indicators.

Continuous monitoring of the etch product diode laser absorption signal with better than 1-s time resolution can be readily achieved by using feedback control to lock the diode laser wavelength to the center of the etch product absorption line. The dual wavelength modulation technique described by Bomse[40] provides this wavelength locking function while simultaneously generating a voltage proportional to the monitored species concentration.

IV. CONCLUSIONS

In this study, infrared lead-salt diode lasers monitored fluorocarbon-based plasmas used for etching of poly-silicon and silicon dioxide wafers in a GEC Reference Cell Reactor. The diode laser sensor was used for *in situ* measurements of neutral CF_2 reactive intermediates and CF_2O etch product. Possible correlations between etch process outcomes and parameters measured by diode laser absorption have been identified. The diode laser measurement of CF_2 concentrations was found to be possibly useful as an etch rate indicator or in characterizing SiO_2 versus poly-Si etch selectivity. In addition, diode laser monitoring of CF_2O during etching of SiO_2 was shown to be a potential end point monitor. Further research and development based on these results are expected to lead to new process control strategies for improved reliability and product yield in plasma etching.

ACKNOWLEDGMENTS

This work was supported by the Advanced Research Projects Agency under Contracts No. DAAH01-91-C-R178 and No. DAAH01-93-C-R126. One of the authors (H.M.A.) acknowledges additional support by SEMATECH under Contract No. 88-MC-502. The views and conclusions contained herein are those of the authors and should not be interpreted as representing the official policies, either expressed or implied, of the Advanced Research Projects Agency or the U.S. Government.

[1]J. Wormhoudt, A. C. Stanton, A. D. Richards, and H. H. Sawin, J. Appl. Phys. **61**, 142 (1987).
[2]A. D. Richards, B. E. Thompson, K. D. Allen, and H. H. Sawin, J. Appl. Phys. **62**, 792 (1987).
[3]N. Itabashi, N. Nishiwaki, M. Magane, S. Naito, T. Goto, A. Matsuda, C. Yamada, and E. Hirota, Jpn. J. Appl. Phys. **29**, L505 (1990).
[4]N. Itabashi, N. Nishiwaki, M. Magane, T. Goto, A. Matsuda, C. Yamada, and E. Hirota, Jpn. J. Appl. Phys. **3**, 585 (1990).
[5]M. Magane, N. Itabashi, N. Nishiwaki, T. Goto, C. Yamada, and E. Hirota, Jpn. J. Appl. Phys. **29**, L829 (1990).
[6]T. Goto, in *GEC 92, 45th Annual Gaseous Electronics Conference*, Boston, MA, 27–30 October 1992, Program and Abstracts (GTE Laboratories, Boston, 1992), p. 82.
[7]J. Wormhoudt, J. Vac. Sci. Technol. A **8**, 1722 (1990).
[8]R. Claude Woods, R. L. McClain, and L. J. Mahoney, in *GEC 91, 44th Annual Gaseous Electronics Conference*, Albuquerque, NM, 22–25 October 1991, Program and Abstracts (University of New Mexico Press, Albuquerque, NM, 1991), p. 57.
[9]H. C. Sun, *et al.*, Appl. Opt. **32**, 885 (1993).
[10]H. C. Sun, V. Patel, E. A. Whittaker, B. Singh, and J. H. Thomas III, J. Vac. Sci. Technol. A **11**, 1193 (1993).
[11]D. S. Bomse, A. C. Stanton, and J. A. Silver, Appl. Opt. **31**, 718 (1992).
[12]J. A. Silver, D. S. Bomse, and A. C. Stanton, Appl. Opt. **30**, 1505 (1991).
[13]J. A. Silver, Appl. Opt. **31**, 707 (1992).
[14]J. Reid and D. Labrie, Appl. Phys. B **26**, 203 (1981).
[15]D. E. Cooper and R. E. Warren, J. Opt. Soc. Am. B **4**, 470 (1987).
[16]J. A. Silver and A. C. Stanton, Appl. Opt. **27**, 1914 (1988).
[17]D. T. Cassidy and J. Reid, Appl. Phys. B **29**, 279 (1982).
[18]D. E. Cooper and C. B. Carlisle, Opt. Lett. **13**, 719 (1988).
[19]H. C. Sun and E. A. Whittaker, Appl. Opt. **31**, 4998 (1992).
[20]P. J. Hargis, Jr., *et al.* Rev. Sci. Instrum. **65**, 140 (1994).
[21]P. A. Miller, H. Anderson, and M. P. Splichal, J. Appl. Phys. **71**, 1171 (1992).
[22]M. P. Splichal and H. M. Anderson, SPIE Proc. **1594**, 189 (1991).
[23]P. B. Davies, P. A. Hamilton, J. M. Elliott, and M. J. Rice, J. Mol. Spectrosc. **102**, 193 (1983).
[24]J. B. Burkholder, C. J. Howard, and P. A. Hamilton, J. Mol. Spectrosc. **127**, 362 (1988).
[25]J. B. Burkholder (private communication).
[26]D. L. Flamm, in *Plasma Etching, an Introduction*, edited by D. M. Manos and D. L. Flamm (Academic, San Diego, 1989), pp. 91-183.
[27]D. L. Flamm and G. K. Herb, in *Plasma Etching, An Introduction*, edited D. M. Manos and D. L. Flamm (Academic, San Diego, 1989), pp. 1-89.
[28]G. S. Oehrlein and Y. H. Lee, J. Vac. Sci. Technol. A**5**, 1585 (1987).
[29]J. Wormhoudt, K. E. McCurdy, and J. B. Burkholder, Chem. Phys. Lett. **158**, 480 (1989).
[30]J. J. Orlando, J. Reid, and D. R. Smith, Chem. Phys. Lett. **141**, 423 (1987).
[31]O. Suto and J. Steinfeld, Chem. Phys. Lett. **168**, 181 (1990).
[32]G. Herzberg, *Molecular Spectra and Molecular Structure: II. Infrared and Raman Spectra of Polyatomic Molecules* (Van Nostrand Reinhold, New York, 1945).
[33]K. Maruyama, A. Sakai, and T. Goto, J. Phys. D **26**, 199 (1993).
[34]L. -M. Buchmann, F. Heinrich, P. Hoffmann, and J. Janes, J. Appl. Phys. **67**, 3635 (1990).
[35]K. R. Ryan and I. C. Plumb, Plasma Chem. Plasma Process. **6**, 231 (1986).
[36]P. J. Hargis, Jr., R. W. Light, and J. M. Gee, in *Laser Processing and Diagnostics*, edited by D. Bauerle, Springer Series in Chemical Physics Vol. 39 (Springer, Berlin, 1984), pp. 526–529.
[37]D. L. Flamm and V. M. Donnelly, Plasma Chem. Plasma Process. **1**, 317 (1981).
[38]L. S. Rothman, *et al.*, J. Quantum Spectrosc. Radiat. Transfer **48**, 469 (1992).
[39]C. Camy-Peyret, J.-M. Flaud, A. Goldman, F. J. Murcray, R. D. Blatherwick, F. S. Bonomo, D. G. Murcray, and C. P. Rinsland, J. Mol. Spectrosc. **149**, 481 (1991).
[40]D. S. Bomse, Appl. Opt. **30**, 2922 (1991).